Electronic Supplementary Material (ESI) for Journal of Materials Chemistry A.


# Supporting Information for

# *Solution processed graphene structures for perovskite solar cells*

Munkhbayar Batmunkh,[a,b] Cameron J. Shearer,[b] Mark J. Biggs,[a,c] and Joseph G. Shapter*,[b]

[a] *School of Chemical Engineering, The University of Adelaide, Adelaide, SA 5005, Australia*

[b] *School of Chemical and Physical Sciences, Flinders University Bedford Park, GPO Box 2100, Adelaide, SA 5001, Australia*

[c] *School of Science, Loughborough University, Loughborough, Leicestershire LE11 3TU, UK*

Fig. S1 shows the Raman spectra of graphene oxide (GO), chemically reduced graphene oxide (CRGO) without and with SDBS surfactant and reveals two typical peaks at 1350 $cm^{-1}$ (D band) and 1592 $cm^{-1}$ (G band). It is well known that the D and G bands indicate the structural defects and $sp^2$ hybridization in carbon materials, respectively. As can be seen from Fig. S1, the D band of CRGO is slightly broad and its intensity is relatively high compared to that of CRGO-SDBS, indicating more defects exist in the CRGO. Moreover, the intensity ratio ($I_D/I_G$) is usually used to determine the defects quantity.[1] Some defects ($I_D/I_G$=0.91) in the GO are expected and is known to be due to the strong oxidization process of graphite.[2] Indeed, the $I_D/I_G$ value of the CRGO-SDBS is 1.04, which is lower than that ($I_D/I_G$=1.23) of CRGO produced without SDBS. This value confirms that the chemical (hydrazine) reduction on GO in the presence of SDBS surfactant creates less defect on the CRGO.

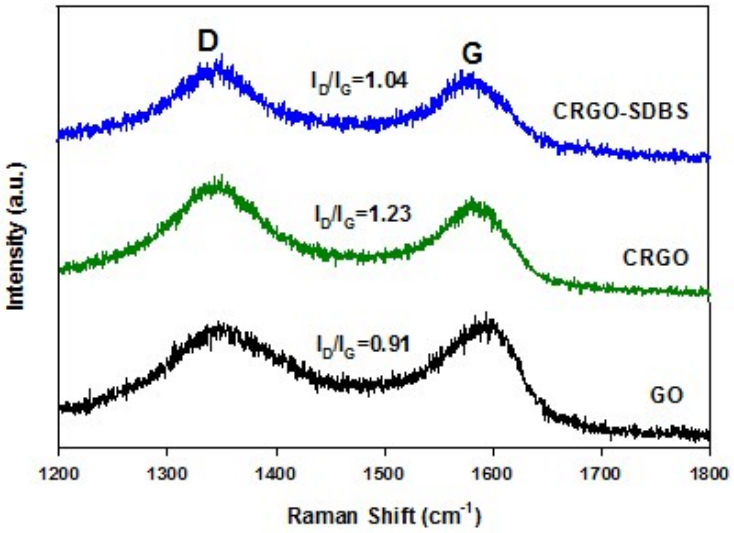


**Fig. S1.** Raman spectra of GO, CRGO without and with SDBS surfactant.

Fig. S2 illustrates curve fitting of the C1s peak in the X-ray photoelectron spectroscopy (XPS) spectra of the samples, namely GO, CRGO-SDBS and RGO-SDBS. The GO spectra can be fit to three individual components, namely C-C at 284.8 eV, C-O at 286 eV and C=O and/or the COO at 287.5 eV. With chemical and thermal reduction the relative area of the C-C peak increased from 24 % for GO to 93 % and 81 %. This result agrees with the ATR-FTIR which showed that oxygen containing functional groups are removed with reduction. The shape of the C1s spectra may be broadened by the presence of SDBS.

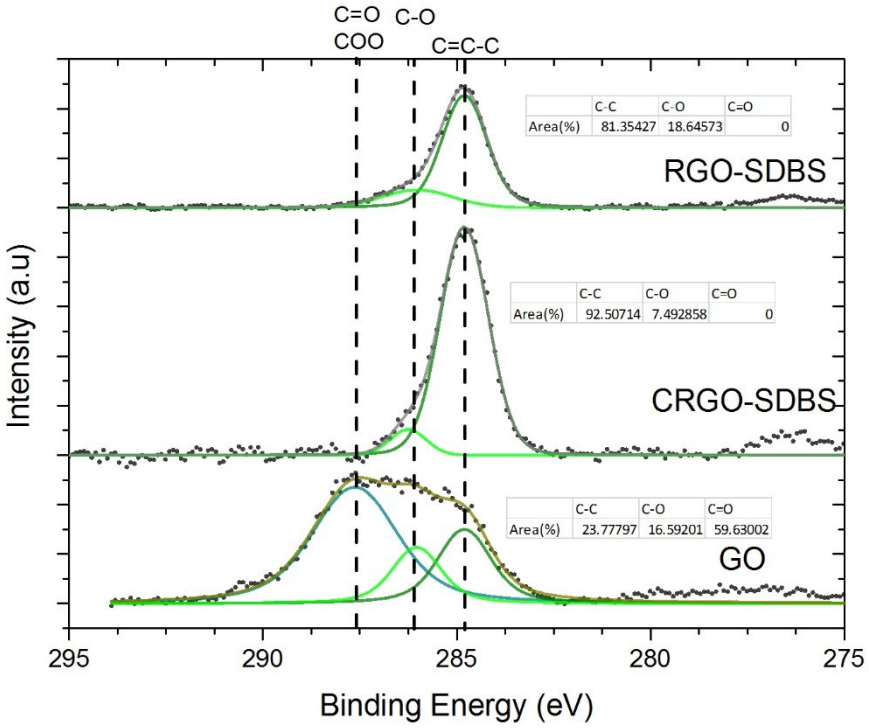


**Fig S2**. Curve fitting of the C1s peak in the XPS spectra of GO, CRGO-SDBS and RGO-SDBS samples.

The thermal stability of SDBS surfactant was studied using thermo-gravimetric analysis (TGA) by (i) heating at 400°C and (ii) heating to 800°C at a rate of 20°C $min^{-1}$ under an inert gas atmosphere. As shown in Fig. S3, very little weight loss was observed for SDBS during heating at a temperature of 400°C for over 1h. This small change in the weight loss of SDBS is in very good agreement with our finding from ATR-FTIR and XPS where slight decrease in the peak intensities was observed. Notably, the main mass loss of SDBS surfactant occurs after annealing at a high temperature (> 500°C). However, our aim in this study was to use low-temperature based thermal process because high temperature annealing is undesired for the future development of flexible solar cells. Although the thermal treatment at 400°C didn't remove the SDBS from the RGO film, the annealing process largely reduced the oxygen containing functional groups and significant improvement in the electrical conductivity of the films can be expected.

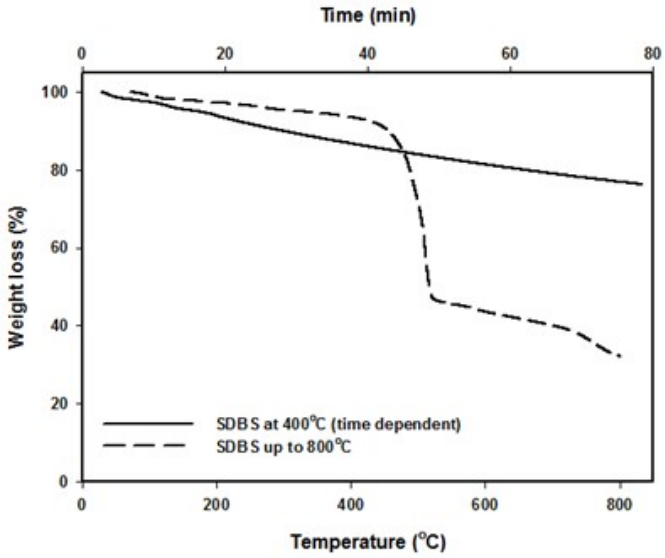


**Fig. S3.** TGA analysis of SDBS surfactant.

Several changes in the optical transmittance of the films have been observed in each treatment. Fig. S4 depicts the light transmittance at wavelength ranging from 400–1000 nm and sheet resistance ($R_s$) of the graphene films. Scheme 1d-g represents the schematic illustration of these films and is shown in Scheme 1.

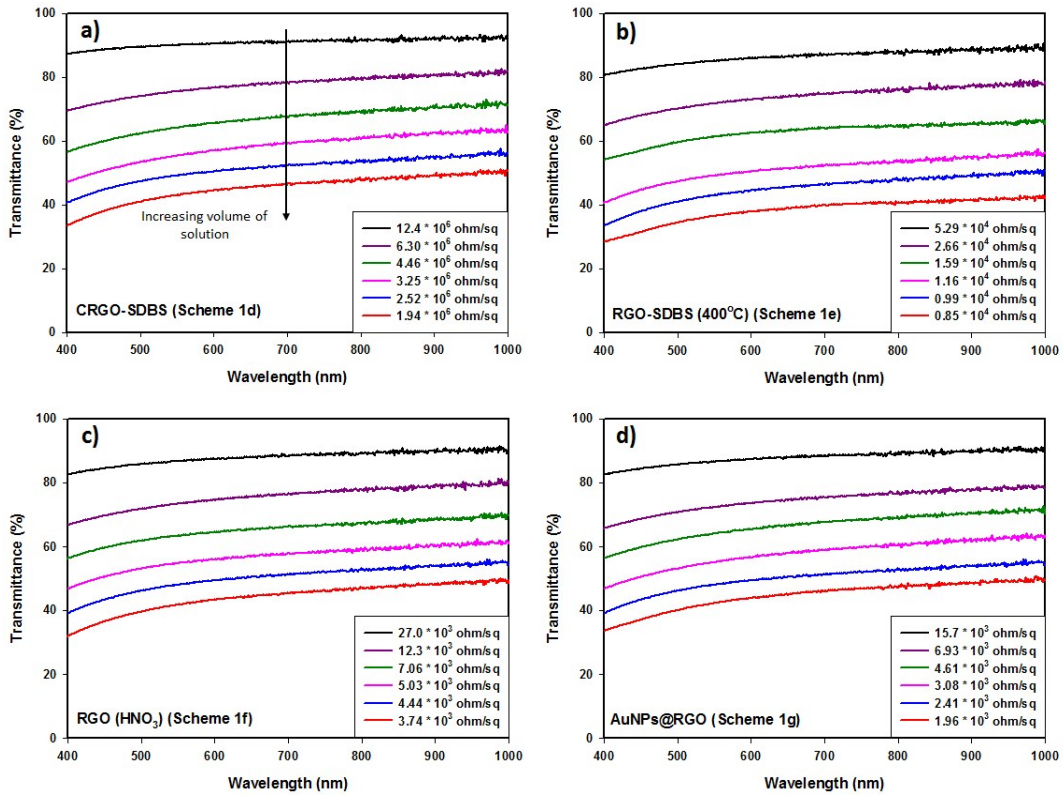


**Fig. S4.** Optical and electrical characteristics of (a) CRGO-SDBS, (b) RGO-SDBS (400°C), (c) RGO ($HNO_3$-treated) and (d) AuNPs-RGO films.

A conventional PSC based on FTO electrode was also fabricated and its *J-V* characteristics are shown in Fig. S5. The structure of the device is also illustrated in the inset of Fig. S5. The FTO electrode based device exhibited $J_{sc}$ of 17.49 mA $cm^{-2}$, $V_{oc}$ of 0.71 V and *FF* of 0.63 and yielding a PCE of 7.82%.

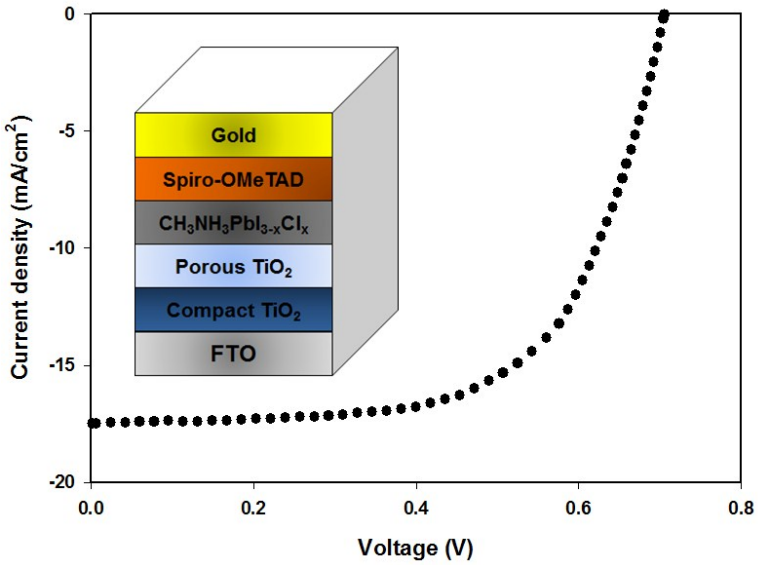


**Fig. S5.** J–V curve of FTO-based PSC. The device structure is shown in the inset.

The stability of PSCs fabricated with FTO-electrode and TCGF electrode was studied for 60 h. After the fabrication of the cells under controlled humidity (< 35%), the cells were stored in ambient conditions (in air and uncontrolled humidity) in the dark for the stability test. The J–V characteristics of the cells were measured in every 12 h. No encapsulation was done for the devices. From Fig. S6 it is clear that the degradation rate of TCGF based cell was very similar to that of a FTO-based device. This indicates that the use of TCGF did not alter the internal decay mechanism of the PSC.

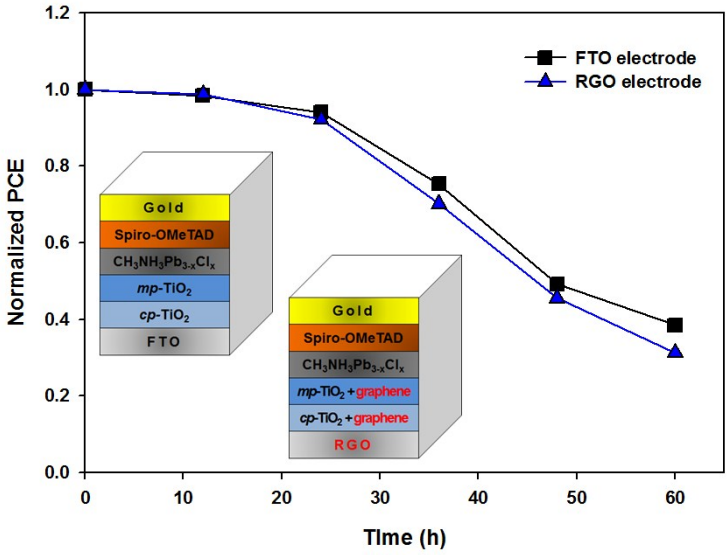


**Fig. S6** Stability of the PSCs fabricated based on FTO-electrode and TCGF (RGO electrode). The device structures are shown in the insets. Initial PCE for FTO-based and TCGF-based cell was 7.41% and 0.77%, respectively.

Section analysis of the AFM images reveals thickness of GO and CRGO-SDBS steps to be in the range of 1-5 nm. This value is typical for such samples when prepared by drop casting. The presented images have identical z-scales.

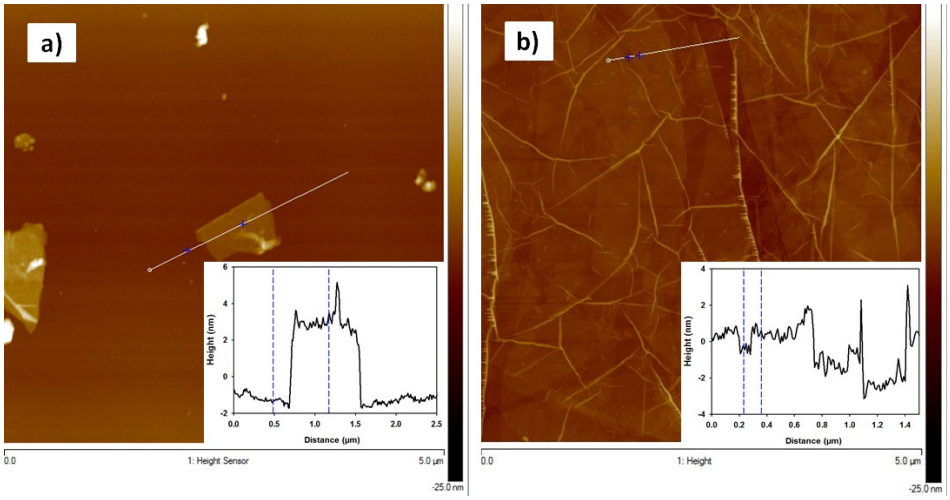


**Fig. S7**. AFM image of CRGO (a) without and with (b) SDBS surfactant. Insets show the thickness measurement using a line profile.

**References**

[1] A. C. Ferrari, D. M. Basko *Nat Nano.* **2013,** 8, 235-246.
[2] Y. Zhu, S. Murali, W. Cai, X. Li, J. W. Suk, J. R. Potts, R. S. Ruoff *Advanced Materials.* **2010,** 22, 3906-3924.